

The interaction of light with an effective moving dispersive medium.

M. Petev,¹ N. Westerberg,¹ D. Moss,¹ E. Rubino,² C. Rimoldi,² S.L. Cacciatori,² F. Belgiorno,³ and D. Faccio^{1,*}

¹*School of Engineering and Physical Sciences, SUPA,
Heriot-Watt University, Edinburgh EH14 4AS, UK*

²*Dipartimento di Scienza e Alta Tecnologia, Università dell'Insubria, Via Valleggio 11, IT-22100 Como, Italy*

³*Dipartimento di Matematica, Politecnico di Milano, Piazza Leonardo 32, 20133 Milano, Italy* *

Intense laser pulses excite a nonlinear polarisation response that may create an effective flowing medium and, under appropriate conditions, a blocking horizon for light. Here we analyse in detail the properties and interaction of light with such laser-induced flowing media, fully accounting for the medium dispersion properties. A first Born approximation scattering model is found to be in excellent agreement with numerical simulations based on Maxwell's equations. Diamond is proposed as a promising candidate medium for future studies of Hawking emission from artificial, dispersive horizons.

Recent developments in the understanding of light propagation have led to evidence that by using intense laser pulses propagating in a nonlinear medium, it is possible to create an effective medium that flows with the same speed as the laser pulse, i.e. at speeds close or even higher than the speed of light in vacuum [1–9]. Indeed, in a medium with a third order (also called “Kerr”) nonlinear polarisation response the refractive index of the medium is given by $n = n_0 + n_2 I(z - vt)$, where n_0 is the background index, n_2 is the nonlinear Kerr index and $I(z - vt)$ is the laser pulse intensity profile, travelling along the z direction with velocity v . In a typical condensed medium, e.g. glass, the maximum amplitude of the laser pulse induced refractive index perturbation is $\delta n_{\max} = n_2 I_{\max} \sim 0.01 - 0.001$. This is sufficient to scatter light, e.g. either light from the laser pulse itself (self-scattering process) or from a second weak probe pulse (induced scattering process). As discussed in the following, there is also interest in the fact that under appropriate conditions one may potentially observe induced scattering (and excitation) of photons that originate from the vacuum state.

One motivation for the interest in the interaction between a moving refractive index variation, δn , and the vacuum state fluctuations lies in the prediction that the δn may be described in terms of a horizon that mimics the event horizon of gravitational black hole [1–7]. Indeed, in the absence of material dispersion, it is possible to write the effective spacetime metric for the moving δn as $ds^2 = c^2 dt^2 + (dr - V dt)^2$. This is equivalent to the Painlevé-Gullstrand metric showing that in the reference frame of the δn the medium is effectively flowing with speed V , that is a Galilean velocity ($-\infty < V < +\infty$) and is determined by n and v . A horizon is formed when $V = c$ [5, 10]. Interaction with the vacuum state leads to the emission of photon pairs that are analogous to Hawking emission from a black hole. Recent measurements claimed the observation of a spontaneous emission from a laser pulse induced moving δn that appeared to have some of the features predicted for the analogue Hawking emission [11, 12]. However, these measurements have not

been considered as conclusive and further evidence is required [13].

In this Letter we investigate in detail the interaction between a moving δn and a probe light pulse. Our analytical and numerical models fully account, without any approximations, for material dispersion, the full shape of the δn and allow a comprehensive analysis of the interaction dynamics for varying δn speed. These studies highlight new and unexpected interaction dynamics between light and a moving or flowing medium: the input probe pulse is scattered into two output modes one with positive and the other with negative comoving frequencies [14]. In agreement with previous studies this leads to amplified emission [15] with the novelty that the noise of this amplifier has a constant temperature for all emitted modes (frequencies) thus resulting in a blackbody emission when seeded from the vacuum state. The blackbody emission is predicted independently of the δn speed although the total photon number increases dramatically close to the condition for which a complete blocking horizon is formed. It is in this regime that we propose a setting for future experiments in diamond that exhibits the required conditions to observe analogue Hawking emission.

Scattering from a moving δn : A soliton propagating in a dispersive medium will shed light through a mechanism known as resonant (or dispersive wave) radiation (RR) [17–20]. This emission may be described as a self-induced scattering process whereby light from the soliton is scattered into a frequency-shifted mode by the self-induced Kerr δn . It was recently shown that a second scattered mode also exists: this mode has negative frequency in the reference frame comoving with the soliton and has been called “negative-frequency resonant radiation” (NRR) [14]. Both these modes are found within the framework of a model that neglects all nonlinear effects and simply considers the soliton δn and models how light is scattered within the first Born-approximation [15]. The model therefore generalises RR and NRR generation beyond soliton physics to include also systems in that do not support solitons (e.g. a 3-dimensional pulse

with transverse spatial dynamics or an intense pulse in the normal group velocity dispersion regime). The scattered amplitudes of the two modes are given by [15]

$$S(\omega_{RR}) = i \frac{v\omega_{RR}^2 n_0}{2c^2 k_z(\omega_{RR})} e^{i \frac{(\omega_{RR} - \omega_{IN})z}{v}} \hat{R}(\omega_{RR} - \omega_{IN}) \quad (1)$$

$$S(\omega_{NRR}) = i \frac{v\omega_{NRR}^2 n_0}{2c^2 k_z(\omega_{NRR})} e^{i \frac{(\omega_{NRR} + \omega_{IN})z}{v}} \hat{R}(\omega_{NRR} + \omega_{IN}) \quad (2)$$

where \hat{R} is the δn Fourier transform and $\omega_{RR, NRR, IN}$ are the RR, NRR and input probe pulse frequencies. A further important result is the generalisation of the photon conservation Manley-Rowe relations to the case of a moving medium [15, 21, 22]: $|RR|^2 - |NRR|^2 = 1$, where $|\cdot|^2$ indicates a photon number normalised to the input photon number. This generalised Manley-Rowe relation implies that the scattering process is actually a photon number amplifier, $|RR|^2 + |NRR|^2 > 1$. This has been confirmed numerically by monitoring the total photon number of a weak seed pulse that interacts with a soliton pulse and is subsequently scattered into RR and NRR modes [15].

Amplification and gain spectrum: In the following we present a series of numerical simulations and a comparison with predictions based on the Born approximation equations (1) and (2) with which we estimate the amplitudes of the RR and NRR waves generated by an input probe pulse interacting with a moving δn , for varying frequency of the input pulse. The numerical simulations were carried out with various codes i.e. using both FDTD [23] and the UPPE [15, 24] model all under the same input conditions and both delivered the same results. In Fig. (1) we show examples obtained with the FDTD code with $\delta n = \delta n_{\max} \exp[-((z - vt)^2/\tau^2)^m]$ where $\delta n_{\max} = 0.01$, τ and m are chosen so that the δn front has a 7 fs rise time. The dispersion is chosen so as to resemble that of diamond and is shown in the figure in (ω', ω) frequency coordinates, where primed quantities indicate that they refer to the comoving reference frame. This is a convenient representation: momentum conservation that must be satisfied during the scattering process, translates in the comoving frame to a frequency, ω' conservation. All modes and relative laboratory frequencies, $\omega_{RR, NRR}$ may therefore be determined from the intersections of the dispersion curve with a horizontal line that passes through the input comoving frequencies, $\pm\omega'_{IN}$ [15].

Figure 1(a) shows the near field, i.e. temporal profile of an input 5 μm wavelength probe beam interacting with the δn in the comoving frame for the generic case in which the δn speed, $v = 1.9 \times 10^8$ m/s is too slow to actually completely block the impinging light for $\delta n_{\max} = 0.01$. We refer to this as the “non-blocking” case: the input light will be transmitted through the δn and will only be partly scattered into the RR and NRR modes that are reflected backwards in the comoving frame (but are

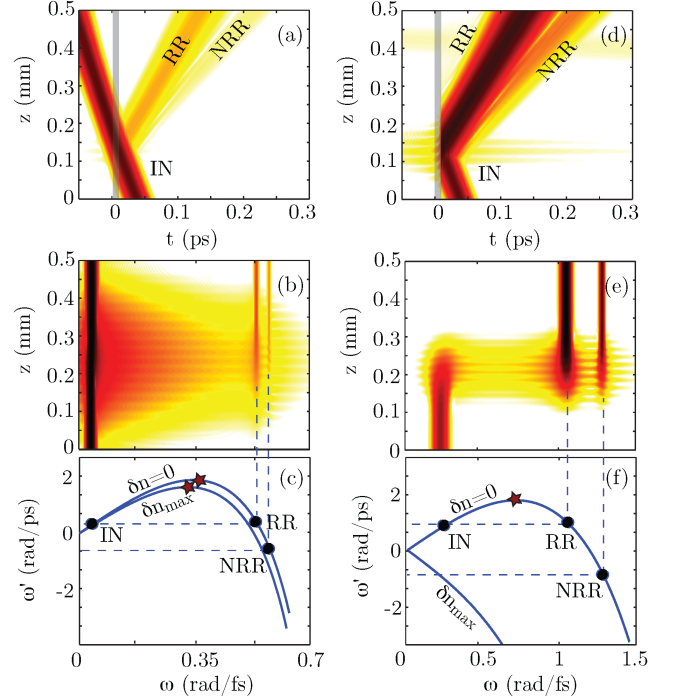


FIG. 1: Example of a numerically simulated interaction of a probe pulse with a moving δn . (a), (b) and (c) show the temporal profile evolution, spectral evolution and relevant dispersion curves, respectively, for the case in which the δn moves too slowly to form a blocking horizon. (d), (e) and (f) show similar figures for a faster δn such that a blocking horizon is formed. The δn rising front is shown as a grey shaded area in (a) and (d). All intensity plots are shown over 4 decades in logarithmic scale. Stars in (c) and (e) indicate the position of the cut-off frequency, ω_{\max} .

travelling forwards in the laboratory frame). This partial conversion is also clear in the frequency spectrum evolution in Fig. 1(b) that shows generated peaks that are in excellent agreement with the frequencies predicted from the dispersion relation in Fig. 1(c).

Figures 1(c), (d) and (e) show similar results but now $v = 2.07 \times 10^8$ m/s has been increased such that the input light pulse is slowed down upon interacting with the δn rising front to the point that its group velocity becomes equal to v , i.e. the δn presents a blocking horizon for light. In this case the input mode is completely converted to the RR and NRR modes.

We now examine the ratio $r = |NRR|^2/|RR|^2$ for varying input frequency. In Fig. 2(a) we show a typical example in logarithmic scale (red points are results from numerical simulations with a non-blocking $v = 1.9 \times 10^8$ m/s, the solid line is a linear fit). The surprising feature here is that r has a clear exponential dependence over more than 8 decades. If we then combine this exponential dependence $r = \exp(-\alpha\omega')$ with the generalised Manley-Rowe relations we find that $|NRR|^2 = 1/[\exp(\alpha\omega') - 1]$.

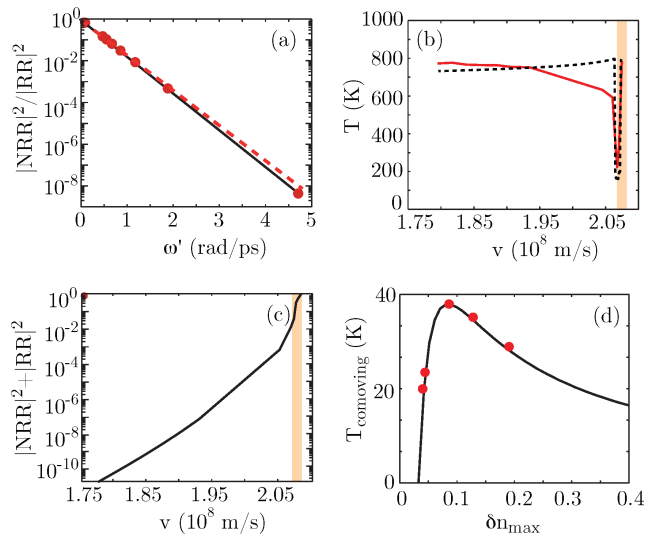


FIG. 2: (a) Numerical simulation for $v = 1.9 \times 10^8$ m/s of $r = |NRR|^2/|RR|^2$ for varying input frequency (dots) and best fit with exponential function (solid line). The Born approximation calculation is shown as a dashed line. (b) Temperature [derived from graphs as in (a)] for varying δn speed - simulations (solid line) and Born approximation model (dashed line). The shaded area indicates speeds for which a blocking horizon is formed. (c) Total normalised photon count for varying speed. (d) Comparison between numerically estimated emission temperature (dots) and theoretical Hawking emission temperature estimated from the δn gradient (solid line) for varying maximum index change, δn_{\max} .

This implies that the NRR mode emission follows a blackbody law with temperature given by $T = \hbar/(k_B \alpha)$. We note that the blackbody dependence is maintained also in the laboratory reference frame, albeit with a temperature $T_{\text{lab}} = T_{\text{comoving}}/[\gamma(1 - vn/c)]$ where $\gamma = 1/\sqrt{1 - (v/c)^2}$ [5]. We note that we can also evaluate r directly from the first Born approximation relations, Eqs. (1)-(2). The same exponential dependence for r is found (shown as a dashed line in Fig. 1(a)) and $r \rightarrow 1$ for $\omega_{\text{IN}} \rightarrow 0$.

In Fig. 2(b) we show the laboratory temperatures obtained from similar curves as shown in Fig. 2(a) for varying δn speeds: the solid line is the result from numerical simulations, the dashed line is the result from the Born approximation equations. The two curves are in overall good qualitative agreement with even a quantitative agreement in terms of the actual temperature values and behaviour as the speed crosses over from the non-blocking to the blocking horizon case (shaded region in the figure). We note a dip in the temperature at the transition from non-blocking to blocking. This is due to the sharp cut-off of the negative mode scattering efficiency when the input frequencies intersect the dispersion curve close to its maximum value, ω'_{\max} as predicted in Refs. [4, 25, 26]. In more detail, in the blocking case only the $\delta n = 0$ dispersion curve [see e.g. Fig. 1(f)] has an ω'_{\max} and suppression

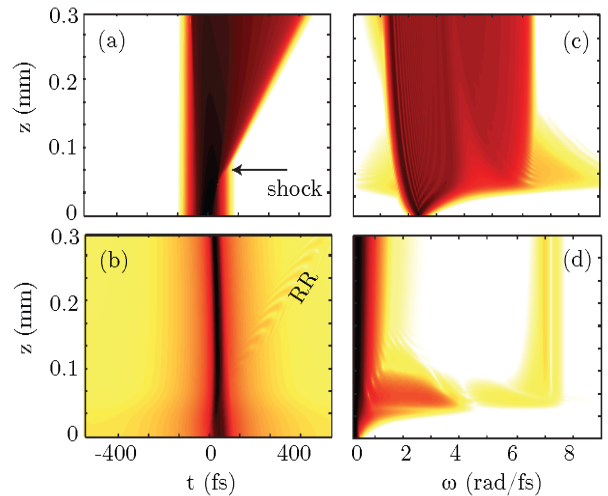


FIG. 3: Numerical simulation of the nonlinear propagation of an 800 nm pump pulse and a co-propagating 15 THz probe pulse (shown in logarithmic scale over 4 decades). Temporal profile evolution of the 800 nm pump pulse (a), and of the THz pulse, (b). The arrow indicates the propagation distance at which a shock front forms on the pump pulse. “RR” indicates emission from the THz pulse scattered from the pump shock front. (c) shows the pump pulse spectral evolution. The THz pulse spectrum (6 decades in logarithmic scale) in (d) shows a clear peak centred around the $\omega' = 0$ point, corresponding to a 7 rad/fs lab frame frequency.

of the NRR mode is not observed as we are probing at relatively low frequencies. As v is decreased, the dispersion curve relative to the internal region of the δn raises up and presents an ω'_{\max} that lies in the same region as the probing frequencies. In agreement with previous studies, NRR generation is then strongly suppressed and the temperature decreases sharply [4, 25, 26]. If v is decreased even further the internal dispersion curve becomes nearly identical to the external curve [similar to Fig. 1(c)] and the two-mode RR-NRR scattering process takes over again with a consequent return of high temperature blackbody emission.

We now note that although the blackbody emission temperature appears to be high across all values of v , the emission efficiency is actually exponentially suppressed as v decreases. In Fig. 2(c) we show the total photon number $|NRR|^2 + |RR|^2$ evaluated from the numerical simulations. As can be seen, this number varies by several orders of magnitude with varying v and is dramatically enhanced in the presence of a blocking horizon.

In the presence of a blocking horizon we may also evaluate the Hawking temperature (at the horizon) according to $T = (1/2\pi)\gamma^2 v |dn/dt|$ [5]. We find that the temperature evaluated both from the numerics and the Born model are in very good agreement with the predicted Hawking temperature. This is shown in Fig. 2(d) where we compare the (comoving) Hawking temperature (solid

curve) and the numerically estimated temperatures (red dots) for δn with a fixed v and varying δn_{\max} . As can be seen, the agreement is excellent over a wide range of values, including δn_{\max} that are experimentally accessible through the nonlinear Kerr effect.

It has already been pointed out that the moving δn acts as an amplifier. From the results presented here it is clear that the amplification increases with the δn speed and reaches maximum efficiency in the presence of a blocking horizon. If the input probe pulse were to be reduced to the level of the quantum noise fluctuations, then the results shown above predict the spontaneous emission of a blackbody spectrum. In other words, the noise of the amplifier is characterised by a temperature that remains constant across all frequencies. This is therefore a very different kind of amplifier with respect to better known examples in optics, e.g. optical parametric amplifiers that have a noise temperature that scales linearly with frequency, $T = \hbar\omega/k_B$ [16]. Finally, we note that the blackbody dependence implies that the amplifier gain scales as $1/\omega'$ for $\omega' \rightarrow 0$. In the comoving frame light is coupled between modes that have a constant or nearly constant $\omega' \sim 0$. Looking at Fig. 1(f) we see that if the input mode has lab. frequency ω close to zero then the output mode will appear at high frequencies, typically in the UV region, in the laboratory frame. The amplifier therefore converts radiation from the low to the high (lab frame) frequency modes and the $1/\omega'$ blackbody divergence will appear as a divergence (or peak) centred at the UV lab frame frequency. The high amplification gain when coupling between $\omega' \sim 0$ modes also indicates possible methods for efficiently observing these scattering effects and possible applications.

For example, in Fig. 3 we show numerical simulations of a weak 15 THz probe (20 μm wavelength) pulse interacting with a Ti:Sapph laser pulse with 800 nm wavelength, 60 fs duration and input intensity 80 TW/cm², propagating in a 500 μm thick diamond sample. These simulations were performed using two UPPE equations, one for the pump and one for the THz pulse that are coupled only through a nonlinear cross-phase modulation term in the THz pulse equation $\propto 2n_2I$ (details of the code can be found e.g. in Ref. [15]). The self-phase modulation term $\propto n_2I$ is included in the 800 nm pump equation but four wave mixing and third harmonic generation have been purposely neglected. There is no blocking horizon for the probe pulse but nevertheless the spectrum clearly shows relatively efficient scattering to the UV that occurs predominantly when a shock front, i.e. the steepest gradient forms on the pump pulse [indicated by an arrow in Fig. 3(a)] in agreement with Eqs. (1) and (2). Most interestingly, the output mode is peaked around the $\omega' \sim 0$, corresponding to a lab frequency of 7 rad/fs (270 nm wavelength). In other words, laboratory reference frame frequencies in the THz or multi-THz region are already sufficiently low to excite the $1/\omega'$ gain of the amplifier.

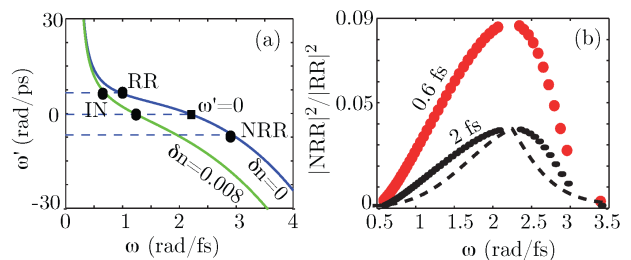


FIG. 4: Numerical simulation of a superluminal δn in fused silica. (a) dispersion relations outside the δn and inside at $\delta n_{\max} = 0.008$. (b) $r = |NRR|^2/|RR|^2$ for two different δn rise times as indicated in the figure. r is peaked at the predicted comoving zero frequency, indicated with a filled square in (a). Dashed curve - result from Born approximation calculation.

This in turn provides indications of the spectral range of the noise fluctuations that may be spontaneously excited by the δn and lead to the spontaneous (i.e. seeded by thermal or vacuum noise) emission peak in the UV. At room temperature, the background blackbody photon mode density at 15 THz is $\sim 10^5$ and thus significantly larger than the quantum vacuum noise mode density equal to just 1/2 a photon per mode: spontaneous emission will be seeded by the thermal background. However, it is sufficient to cool the diamond sample to ~ 30 K to invert the situation such that thermal fluctuations are dominated by more than 1 order of magnitude by quantum vacuum noise.

As a final comment, we note that superluminal speeds may be obtained using Bessel pulses: in diamond if $v > c$ the dispersion curves both inside and outside the δn resemble the curve for δn_{\max} in Fig. 1(f) so there is only one intersection point $\omega' = \omega'_{\text{IN}}$. Therefore only one mode (NRR) will be excited and there will be no amplification. However, in fused silica glass the dispersion relation exhibits a resonance in the infrared that allows coupling to two output RR and NRR modes or between two $\omega' = 0$ modes. The dispersion relations for fused silica relative to recent experiments using such Bessel-induced superluminal δn are shown in Fig. 4(a). If the probe input pulse starts from *inside* the δn , then the pulse will start to lag behind, exit the δn and, when traversing the δn gradient it will excite RR and NRR output modes. If we repeat the procedure outlined above, i.e. we repeat the simulations for varying input wavelength and monitor $r = |NRR|^2/|RR|^2$, we obtain the results in Fig. 4(b) that shows curves for two different δn rise times (0.6 fs and 2 fs). The dashed curve shows the result obtained for the 2 fs gradient pulse using the Born approximation and is in good agreement with the numerics. In all cases, we see that r is peaked at the $\omega' = 0$ frequency point on the $\delta n = 0$ dispersion curve [indicated with a solid square in (a)]. This indicates that spontaneous emis-

sion will have maximum gain at this “zero-frequency” mode, in agreement with measurements of spontaneous emission reported in Ref. [11]. Although a quantitative comparison with analogue Hawking emission is somewhat thwarted by the absence of a blocking horizon, which in turn poses a difficulty in making a direct comparison with a Hawking temperature [13], we see that the gain peak at $\omega' \sim 0$ in fused silica glass is essentially of the same nature of that observed in the blocking (and non-blocking) horizon case analysed in diamond. However, the latter material does seem more appropriate for future experiments aimed at observing and studying a faithful analogue of Hawking emission.

Conclusions: a numerical and analytical evaluation of the interaction of a weak light pulse with a steep refractive perturbation leads to the emission of two output modes. This interaction may lead to an increase of the overall photon number, i.e. amplification of the input light pulse at the expense of the moving δn . If the δn is generated through the nonlinear Kerr effect by an intense pump pulse, then energy will be extracted from this pump pulse. The moving δn may be tuned so as to form a blocking horizon for incoming light modes. In this regime, the process is greatly enhanced and in diamond-like media (i.e. media with no resonances at infrared wavelengths) the emission bears all the attributes of analogue Hawking radiation, namely a blackbody emission originating from the excitation of two coupled modes at a blocking, yet dispersive horizon. Optical horizons have been proposed for all-optical transistors [27] but other applications of an effective moving medium to be considered in future work could be relatively efficient THz detection by frequency conversion in diamond (even without a horizon, as shown in Fig. 3) or generation of squeezed vacuum states in the UV region.

D.F. acknowledges discussions with I. Carusotto, S. Finazzi and financial support from the Engineering and Physical Sciences Research Council EPSRC, Grant EP/J00443X/1 and from the European Research Council under the European Union’s Seventh Framework Programme (FP/2007-2013) / ERC Grant Agreement n. 306559.

* Electronic address: d.faccio@hw.ac.uk

- [1] T. G. Philbin, C. Kuklewicz, S. Robertson, S. Hill, F. König, and U. Leonhardt, *Science* **319**, 1367 (2008).
 [2] D. Faccio, *Contemp. Phys.*, **53**, 97 (2012).

- [3] D. Faccio, S. Cacciatori, V. Gorini, V.G. Sala, A. Averchi, A. Lotti, M. Kolesik, J.V. Moloney, *EuroPhys. Lett.*, **89**, 34004 (2010).
 [4] S. Finazzi, I. Carusotto, *Phys. Rev. A*, **87**, 023803 (2013).
 [5] F. Belgiorno, S.L. Cacciatori, G. Ortenzi, L. Rizzi, V. Gorini, D. Faccio, *Phys. Rev. D*, **83**, 024015 (2011).
 [6] S. L. Cacciatori, F. Belgiorno, V. Gorini, G. Ortenzi, L. Rizzi, V.G. Sala, D. Faccio, *New J. Phys.*, **12**, 095021 (2010).
 [7] C. Barceló, S. Liberati, M. Visser, *Living Rev. Relativity*, **14**, 3 (2011).
 [8] A. Guerreiro, A. Ferreira, J.T. Mendonça, *Phys. Rev. A*, **83**, 052302 (2011).
 [9] F. Belgiorno, S.L. Cacciatori, G. Ortenzi, V.G. Sala, D. Faccio, *Phys. Rev. Lett.*, **104**, 140403 (2010).
 [10] A. J. S. Hamilton, J. P. Lisle, *Am. J. Phys.*, **76**, 519 (2008).
 [11] F. Belgiorno, S.L. Cacciatori, M. Clerici, V. Gorini, L. Rizzi, G. Ortenzi, E. Rubino, V.G. Sala, D. Faccio, *Phys. Rev. Lett.*, **105**, 203901 (2010).
 [12] E. Rubino, F. Belgiorno, S.L. Cacciatori, M. Clerici, V. Gorini, G. Ortenzi, L. Rizzi, V.G. Sala, M. Kolesik and D. Faccio, *New J. Phys.*, **13**, 085005 (2011).
 [13] R. Schützhold, W. G. Unruh, *Phys. Rev. Lett.*, **107**, 149401 (2011).
 [14] E. Rubino, J. McLenaghan, S.C. Kehr, F. Belgiorno, D. Townsend, S. Rohr, C.E. Kuklewicz, U. Leonhardt, F. König, D. Faccio, *Phys. Rev. Lett.*, **108**, 253901 (2012).
 [15] E. Rubino, A. Lotti, F. Belgiorno, S.L. Cacciatori, A. Couairon, U. Leonhardt, D. Faccio, *Scient. Rep.*, **2**, 932 (2012).
 [16] W.H. Louisell, A. Yariv, A.E. Seigman, *Phys. Rev. A*, **12A**, p. 1646 (1961).
 [17] P.K.A. Wai, C.R. Menyuk, Y.C. Lee, and H.H. Chen, *Opt. Lett.*, **11**, 464 (1986).
 [18] N. Akhmediev, M. Karlsson, *Phys. Rev. Lett.* **51**, 2602 (1995).
 [19] D.V. Skryabin, and A.V. Yulin, *Phys. Rev. E*, **72**, 016619 (2005).
 [20] J.M. Dudley, G. Genty, S. Coen, *Rev. Mod. Phys.*, **78**, 1135 (2006).
 [21] L.A. Ostrovskii, *Soviet Phys. JETP*, **34**, 293 (1972).
 [22] Y.A. Kravtsov, L.A. , Ostrovskii, N.S. Stepanov, *Proc. IEEE* **62**, 1492 (1974).
 [23] A. Taflove, S.C. Hagness, “Computational Electrodynamics: The Finite-Difference Time-Domain Method” (Artech House Ed., London, 2005).
 [24] M. Kolesik, J. V. Moloney, *Phys. Rev. E*, **70**, 036604 (2004).
 [25] J. Macher, R. Parentani, *Phys. Rev. D*, **79**, 124008 (2009).
 [26] A. Recati, N. Pavloff, and I. Carusotto, *Phys. Rev. A*, **80**, 043603 (2009).
 [27] A. Demircan, Sh. Amiranashvili, G. Steinmeyer, *Phys. Rev. Lett.* **106**, 163901 (2011).